Stanford Exploration Project, Report 75, November 17, 1997, pages 147–167

Stanford Exploration Project, Report 75, November 17, 1997, pages 147–167

Kirchhoff wave-equation datuming with irregular acquisition topography

Dimitri Bevc[1]

keywords: *velocity, algorithm, continuation, prestack, land, acquisition*

ABSTRACT

Seismic data gathered on land is distorted by irregular acquisition topography. Most seismic imaging algorithms are applied to data which is shifted to a planar datum. In regions of mild topography a static shift is adequate to perform this transformation, however as the necessary shift increases in magnitude, the static approximation becomes inadequate. In this situation a procedure based on wave-equation extrapolation is more appropriate than static shift. After describing the Kirchhoff datuming algorithm I apply it to a deep-water marine data set and to synthetic land data. The land data examples demonstrate that wave-equation datuming is more appropriate than static shift in regions of large topographic relief.

INTRODUCTION

The effect of irregular acquisition topography is that it distorts seismic data. This is a serious problem in mountainous regions where there is extreme topographic relief along seismic lines. Wave-equation extrapolation provides a useful method of transforming data to a planar datum and then determining the near-surface velocity structure. This eliminates the distortion caused by the topography and allows standard processing methods such as velocity analysis, DMO, and migration to be applied.

Shtivelman and Canning (1988) show how data can be continued through known velocity structures using an asymptotic form of the Kirchhoff integral equation. McMechan and Chen (1990) implicitly include effects due to topography and near-surface velocity variation in prestack migration. In order for these methods to work, the near-surface velocity must be known. The more general situation I outlined in a previous report (1992) is one for which the near-surface velocity structure is unknown. In this situation I propose upward continuing the data to some planar datum above the topography with some fictitious extrapolation velocity. This should unravel the dis-

[1]**email:** not available

tortions caused by the irregular acquisition topography and allow standard imaging techniques to be applied to the data.

The proposed method is similar to wave-equation datuming applied to marine data to compensate for irregular water-bottom topography (Berryhill, 1979, 1984, 1986; Yilmaz and Lucas, 1986). In the marine case, the data are downward continued to the water-bottom with the water velocity, and then upward continued with the water-bottom velocity. This removes the distortions due to the irregular water-bottom.

Land data is much like the marine data which has been continued to the water-bottom. I propose that the land data be extrapolated upward to some flat datum with an appropriate velocity. Once the data have been extrapolated to the flat datum, standard velocity analysis methods may be used to determine the near-surface velocity. Processing and imaging can be performed at the new datum or the data can be downward continued to some lower datum.

In this paper I present the implementation of a Kirchhoff datuming algorithm and apply it to real marine data and to synthetic land data. This paper presents the new concept that Kirchhoff datuming can be cast as conjugate pairs for upward and downward continuation. This property is exploited by Zhang and Claerbout (1992) as the basis for an interpolation algorithm. Ji and Claerbout (1992) and Popovici (1992) consider the conjugacy of Fourier domain wave-equation datuming.

I analyze the effect of irregular topography on zero–offset and pre-stack data. Forward models are generated by Kirchhoff modeling and migrated by Kirchhoff migration. Static shift is shown to be inappropriate but wave-equation datuming followed by migration produces a good image. Wave-equation datuming provides a way of extrapolating a distorted wavefield to a planar datum without knowledge of the near surface velocity structure. Once the data is at the planar datum, the velocity structure can be determined.

KIRCHHOFF DATUMING

Berryhill (1979) gives the following expression for the upward continuation of a scalar wavefield:

$$U(0,z,t) = \frac{1}{\pi}\int_{-\infty}^{\infty} dx \frac{z}{c}\frac{1}{r_x} Q(t - \frac{r_x}{c}) \tag{1}$$

where $U(0,z,t)$ is one trace of the upward continued wavefield at datum elevation z and lateral position $x = 0$. The function Q is a time delayed filtered version of the input traces on the original datum. The derivation of this equation is reviewed in the Appendix. Two major assumptions go into the derivation of equation (1):

- The wavefield is two-dimensional and does not vary perpendicular to the seismic line.
- The data are collected on a planar surface.

Despite these assumptions, the algorithm based on this integral produces satisfactory results. The assumptions are locally valid for non-planar datums.

For a wavefield transformation from one datum $U(x, z = z_1, t)$ to another $U(x, z = z_2, t)$ (Figure 1) the discretized form of equation (1) is a summation. Each individual trace $U_j(t)$ comprising $U(x, z = z_2, t)$ is calculated by performing the sum:

$$U_j(t) = \sum_j \triangle x_i \cos\theta_i \frac{t_i}{r_i} Q_i(t - t_i) \tag{2}$$

where $Q_i(t - t_i)$ is a filtered input trace recorded at location i along the lower datum and delayed by traveltime t_i. This filtering operation is described in the Appendix. The effect of the filtering operation is to perform a phase-shift of the traces input to the datuming algorithm. $\triangle x_i$ is the input trace interval, θ_i is the angle between the normal to the surface at $z = z_2$ and the line r_i connecting U_j and U_i.

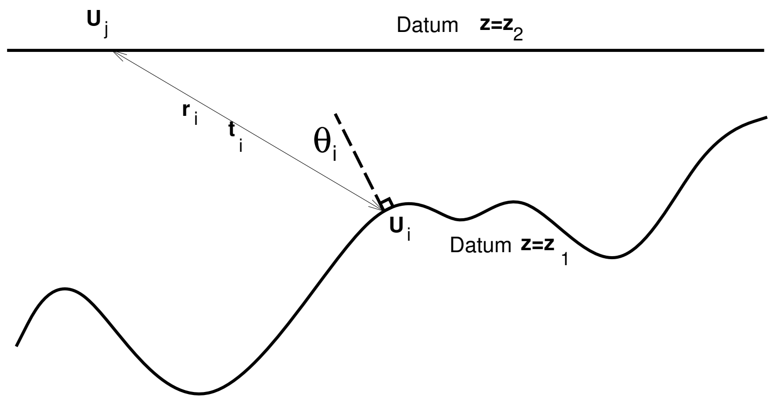

Figure 1: Geometry for the continuation of a wavefield between an irregular topography and a planar datum. dimitri4-datumfig2 [NR]

Equations (1) and (2) are used for upward continuation. For downward continuation the conjugate process is used. The sum is performed first and then the output traces are crosscorrelated with the $\tan\psi$ filter described in the Appendix.

The program for upward and downward continuation is illustrated by the following pseudo-code:

```
loop over j {
loop over i {
     shift = time shift between input and output trace
     if ( conj != 0 )
          Q = down [convolve] filter
     loop over time {
          if ( conj == 0 )
               Q(time-shift,i) = Q(time-shift,i) + up(time,j)
          else
```

```
            up(time,j)          = up(time,j)   + Q(time-shift,i)
                 }
  if ( conj == 0 )
       down = up [crosscorrelate] filter
  }}
```

The notation in the pseudo-code is consistent with Figure 1. The data on the upper datum $z = z_2$ corresponds to index `j` and the data on the lower datum $z = z_1$ corresponds to index `i`. For `conj!=0` the data are upward continued from `down` to `up` and for `conj==0` the data are downward continued.

The actual code used to perform the datuming in this paper is complicated by calculation of geometrical parameters which arise due to non-planar datums and by the incorporation of anti-aliasing. Since the datuming algorithm is based on an integral equation solution it is susceptible to operator aliasing. This is taken care of by calculating triangular smoothing functions along the operator trajectory in a manner analogous to Claerbout (1992).

MARINE DATA EXAMPLES

I apply the datuming algorithm to marine data to illustrate the effectiveness of the datuming algorithm and to point out the similarity between marine data continued to the ocean bottom and land data collected on an irregular surface.

The near-offset section of a high quality marine data set is displayed in Figure 2. This is the offshore southern California data used by Fowler (1988). The complex structure in the center of the line causes prominent diffraction events. The dashed line in Figure 2 represents a datum along the ocean floor defined by the first break picks. The near-offset is 66 m so I treat the data as if it were zero-offset and input it to the datuming algorithm.

The downward continued data are displayed in Figure 3. The diffractions have now partially collapsed but they look somewhat deformed due to the dipping and undulating seafloor datum. The prominent seafloor multiple is now the same shape and at the same time delay as the seafloor primary of Figure 2. This corresponds to an arrival reflecting from the ocean surface. The lower left portion of Figure 3 contains no events below about 1.2 s because the data input to the datuming program only extend to 2 s and the seafloor in this region is at about 0.8 s. The downward continued data appear to have a lower frequency content than the original data.

Yilmaz and Lucas (1986) and Berryhill (1986) perform downward continuation with the water velocity as I have done here in regions with severe water bottom topography and high velocity contrast between the water and the sediments. They then upward continue the data using the sediment velocity in order to eliminate distortions due to ray-bending. For the data set used here the velocity contrast between the water and the sediments is small so this procedure is not applied.

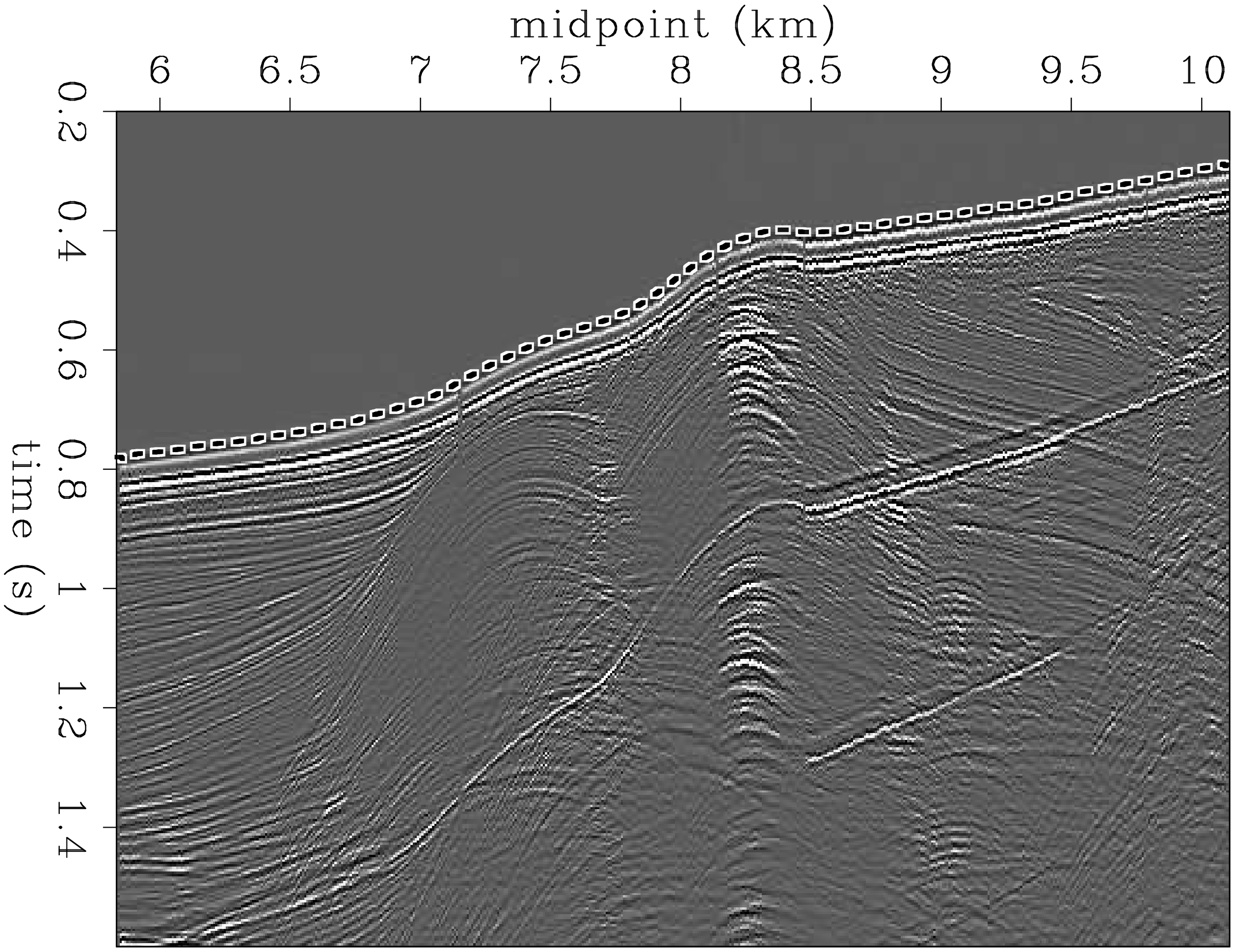

Figure 2: Offshore California near-offset data with first break picks overlaid. dimitri4-picks [NR]

Except for the event due to the surface reflection, the downward continued data may be thought of as being similar to land data acquired on an irregular surface. The distortion of the diffractions would be the same in both cases. The process of upward continuing the data back to sea level is analogous to upward continuing land data to some arbitrary datum above the highest topographic relief. Figure 4 shows the data which have been continued back up to the surface from the ocean bottom. The partially collapsed and distorted diffractions have been faithfully restored to the same state as in Figure 2; however, Figure 4 has lower frequency content than the original data. This may be due to effects of the anti-aliasing.

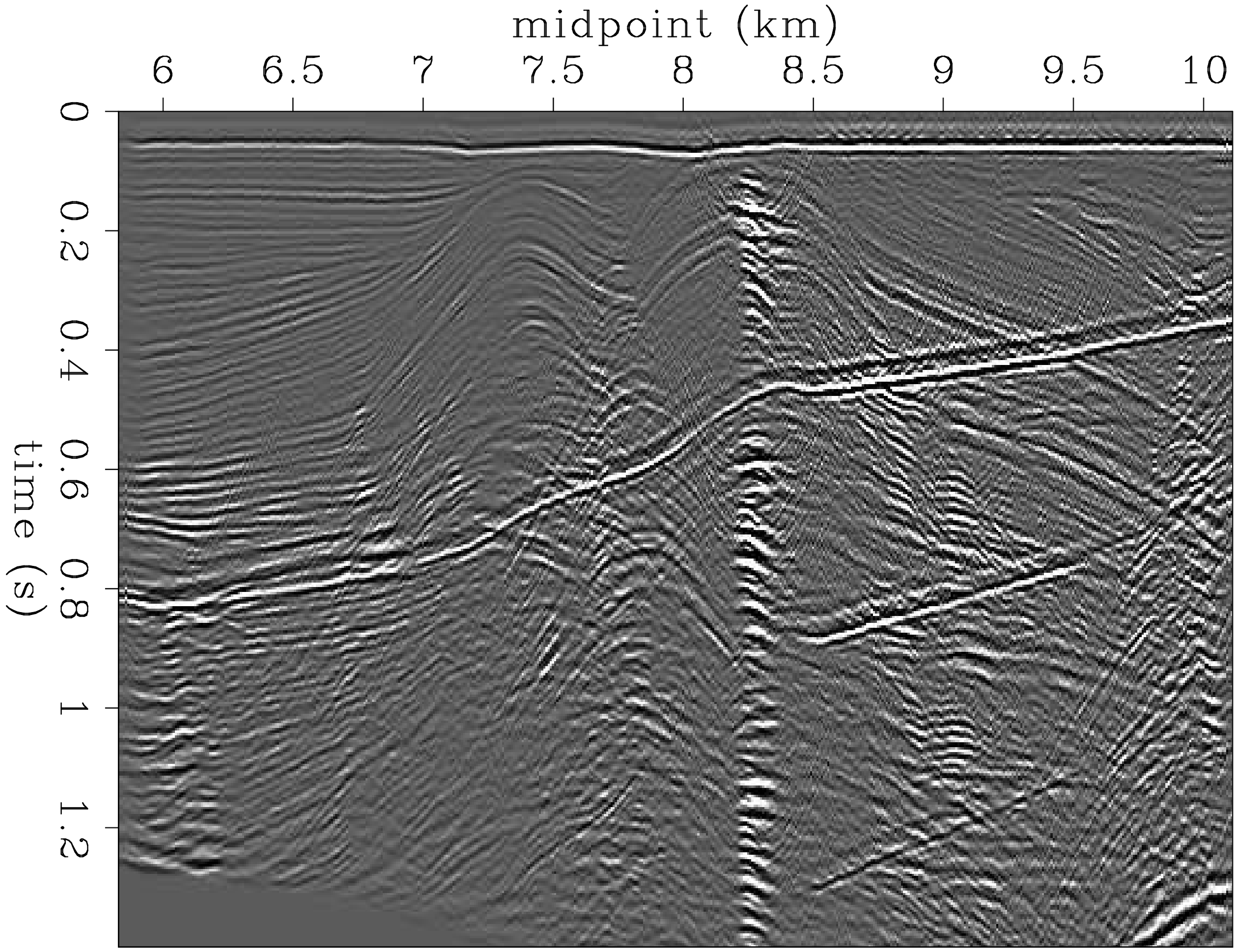

Figure 3: Offshore California near-offset data downward continued to the ocean bottom. dimitri4-seafloor [NR]

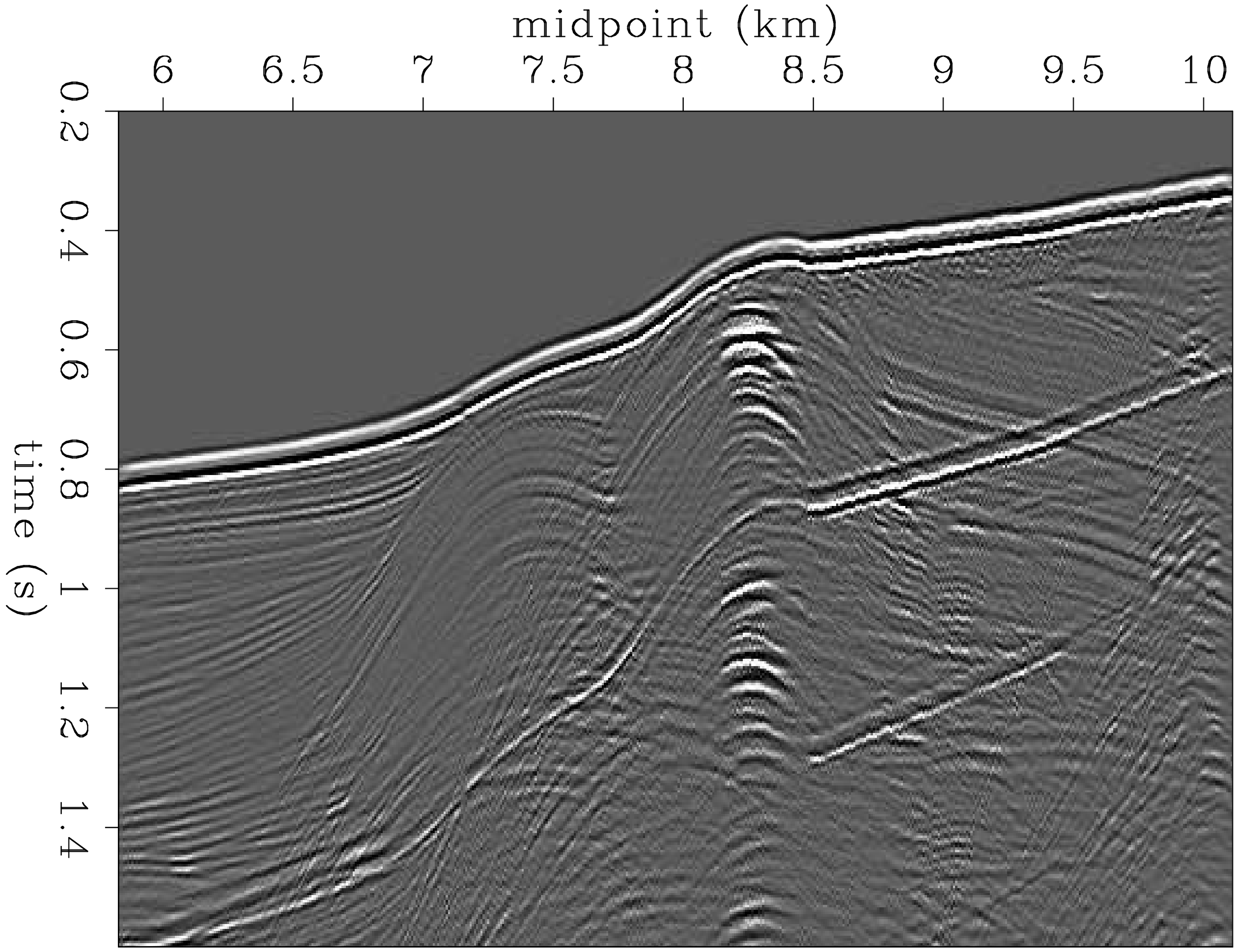

Figure 4: Offshore California near-offset data upward continued back to the surface. dimitri4-sealevel [NR]

IRREGULAR TOPOGRAPHY

Kirchhoff Modeling and Migration with Topography

A zero-offset Kirchhoff modeling and migration program is used to generate synthetic data on an irregular surface. The algorithm is similar to `trimo()` (Claerbout, 1992) but it incorporates topography. The effect of topography is examined by performing static shifts, wave-equation datuming and migration on the zero-offset synthetics. In actual practice data must be datumed pre-stack; However, the zero-offset case is examined here because it is a first step in gaining intuition into the problems encountered with irregular topography and because it is easy to visualize what the zero-offset synthetics should look like. Pre-stack datuming is discussed in a subsequent section.

The model used in this section consists of an anticline, a syncline, and two point diffractors in a constant velocity media. The medium velocity is 2 km/s. The topography is modeled as a cosine shaped mountain 200 m high (Figure 5). The effect of the mountain is to create a low frequency undulation which completely distorts the synthetic data (Figure 6a). The data are migrated using the conjugate of the program which created the synthetic (Figure 6b). This type of migration requires knowledge of the subsurface velocity structure. The problem with many land data sets is that the topography distorts the data so much that it is not possible to pick coherent reflection events or to estimate velocity.

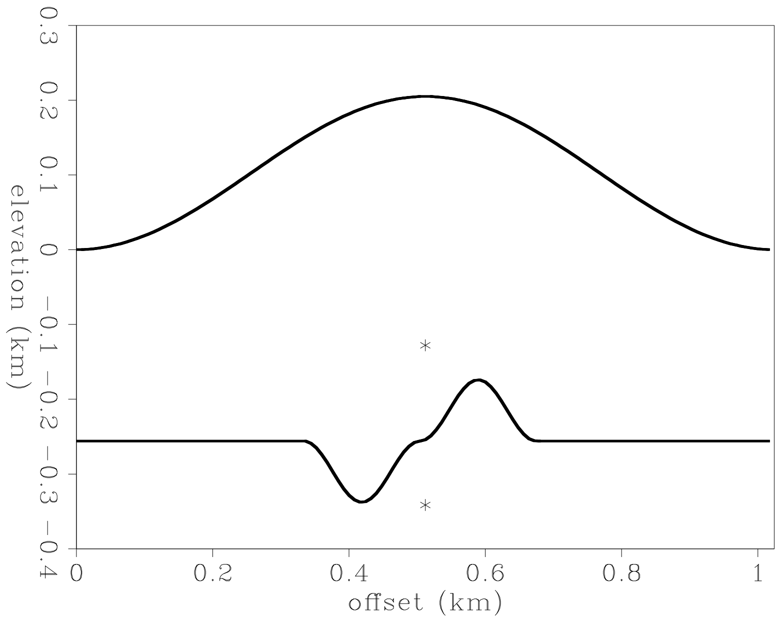

Figure 5: Topography and subsurface structure used to generate the zero-offset synthetic data. dimitri4-model [ER]

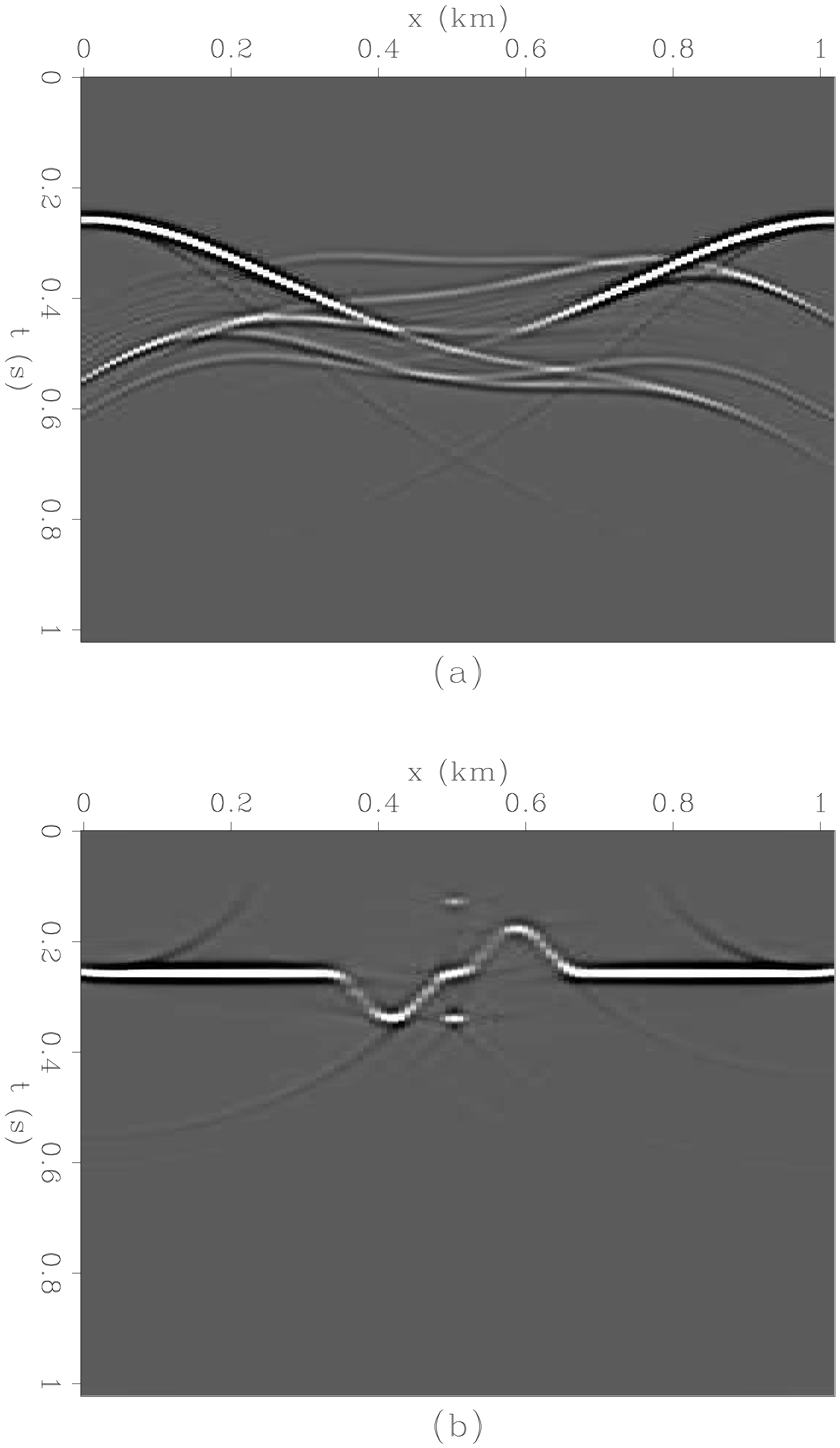

Figure 6: (a) The zero-offset synthetic data are distorted by the irregular acquisition topography. (b) The synthetic data are migrated using an implicit topographic correction. This requires knowledge of the subsurface velocity structure. dimitri4-syn [ER]

Static Shift and Wave-Equation Datuming

The most common form of datuming is to perform static shifts of data traces. This is adequate for regions where the near surface raypaths are nearly vertical and where the shifts are small. The static shift method is commonly applied to correct for near surface velocity variations due to weathering layers, for mild topographic effects, and for differences in shot and geophone elevation. In this section I demonstrate that static shift is inappropriate when the shift is too large because the raypaths are not vertical. I show that downward continuing the data with the wave-equation is a better alternative than static shift when the velocity of the medium is known. Upward continuing the data produces a wavefield which can be correctly imaged although some of the high time-dip information is lost.

Figure 7a shows the migration of the synthetic data from Figure 6a after static shift down to a level datum at the base of the mountain. Similarly, Figure 7b shows the migration of the same synthetic data after shifting upward to a planar datum just above the mountain. In both cases the wavefield is distorted so much by the static shift that the migration fails. The same type of failure occurs for pre-stack data if large static corrections are performed before velocity analysis or any other wave-equation based processing.

The failure of migration or velocity analysis after static shift can be easily understood. Kirchhoff time migration of data collected on a planar surface can be thought of as summation along hyperbolic trajectories (Schneider, 1978). Figure 8a shows the synthetic data after static shift. This is the data which produced the poor migration in Figure 7b. The diffraction curve from the upper point scatterer is non-hyperbolic and therefore does not collapse to a point after migration. Figure 8b is the same synthetic data propagated upward with the wave-equation datuming algorithm. The diffraction curve due to the scatterer is now hyperbolic. All of the events in Figure 8b are properly positioned.

Figure 9 shows the migrations of the zero-offset synthetic data after (a) downward continuation and (b) upward continuation. Both produce acceptable images although the image after downward continuation is better since the steep dips are present. When the wavefield is upward continued some of the steep dip information is lost due to limited aperture. Despite these aperture effects the syncline, anticline and diffractors are clearly resolvable in Figure 9b.

Although the result of Figure 9b requires knowledge of the subsurface velocity structure in order to perform the migration, the upward continuation process applied before the migration does not. This implies that data can be upward continued as in Figure 8b with any reasonable velocity. The upward continued data satisfy the wave-equation.

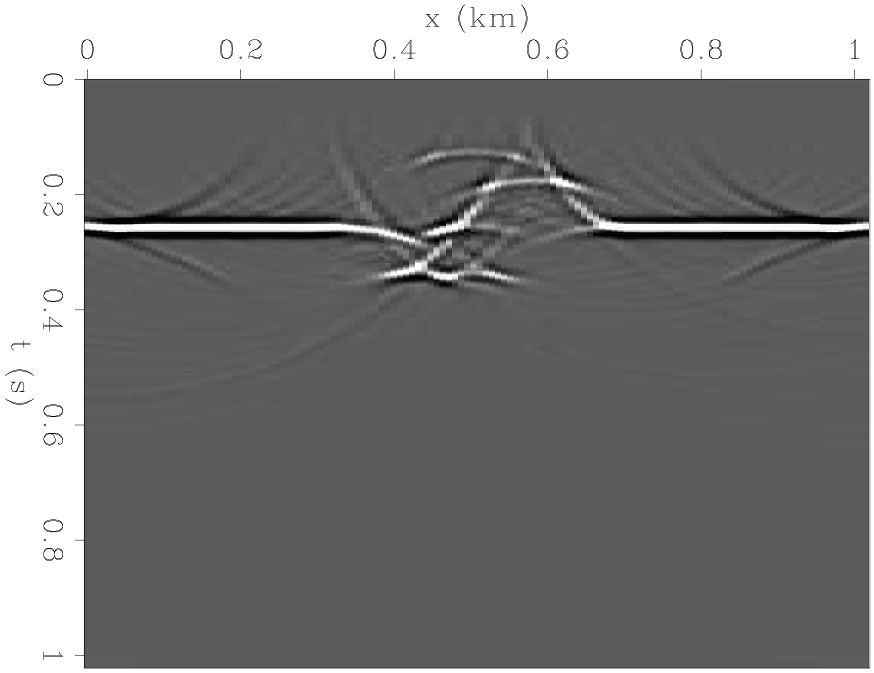

(a)

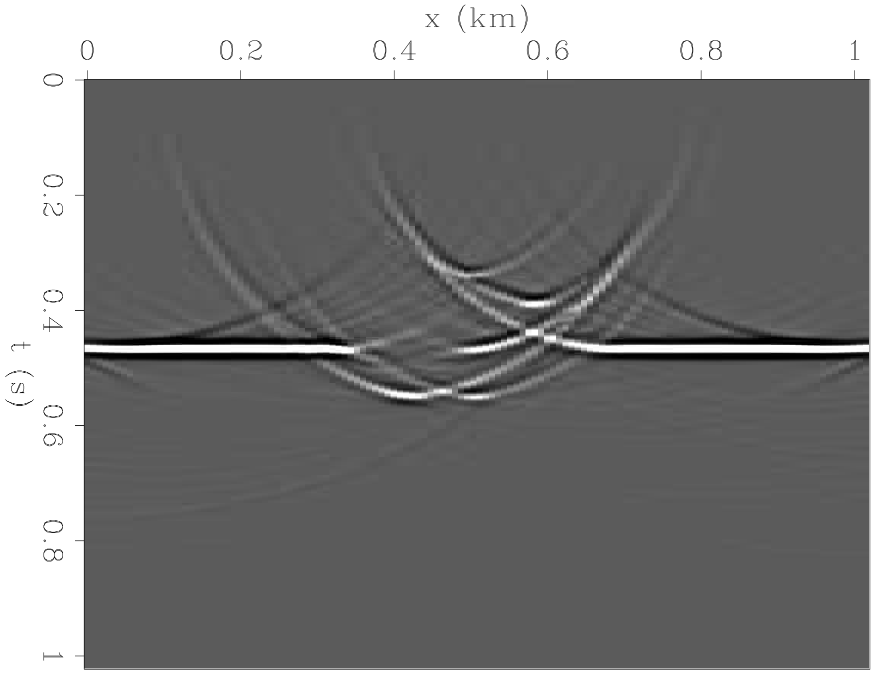

(b)

Figure 7: (a) Static shift downward followed by migration and (b) static shift upward followed by migration. The process of static shift distorts the wavefield so that migration fails. dimitri4-statmig [ER]

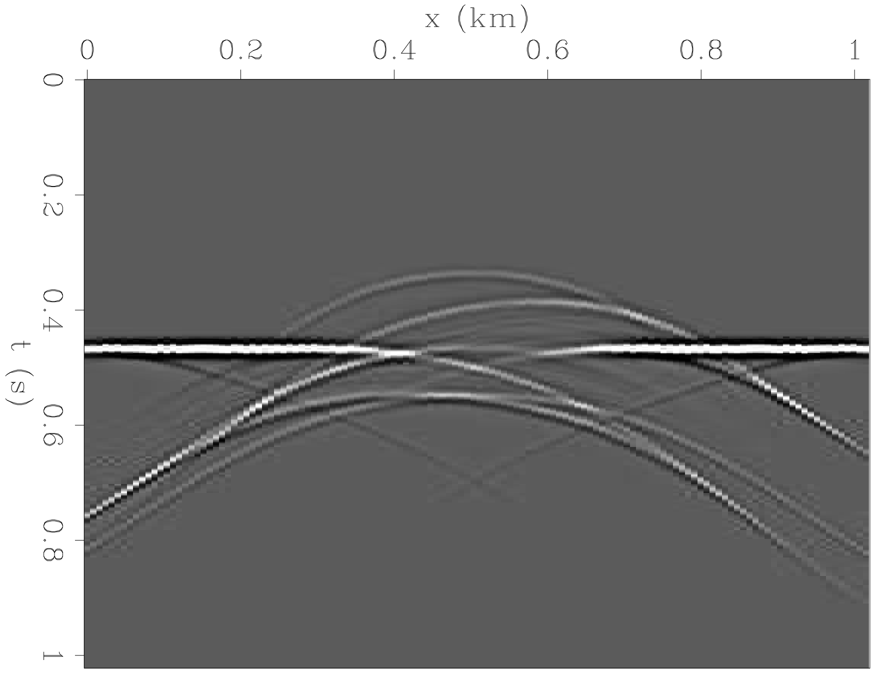

(a)

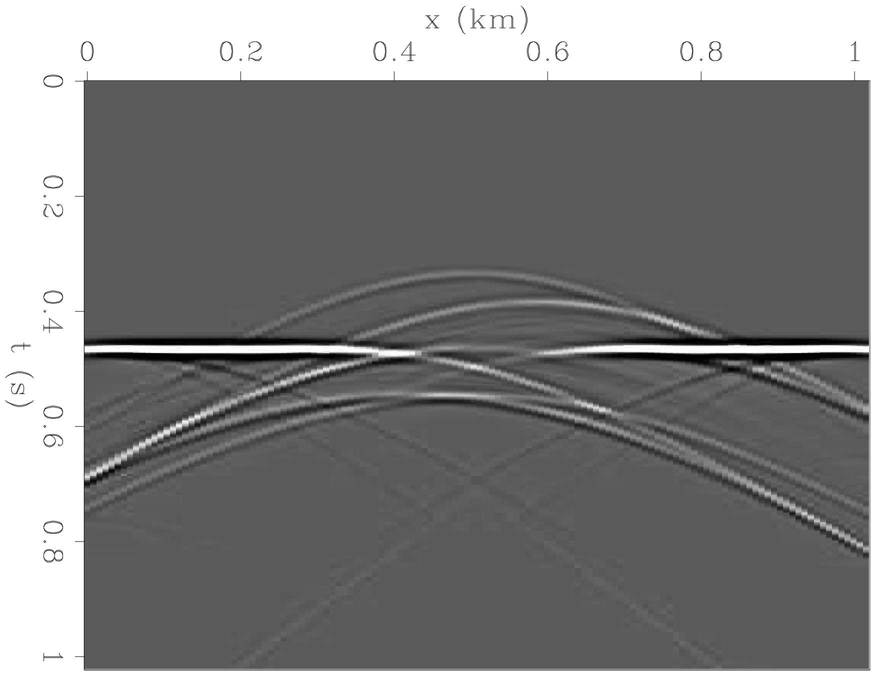

(b)

Figure 8: (a) Static shift upward. (b) Datuming by wave-equation extrapolation upward. Note the difference in curvature of the diffracted events. $\boxed{\text{dimitri4-statdat}}$ [ER]

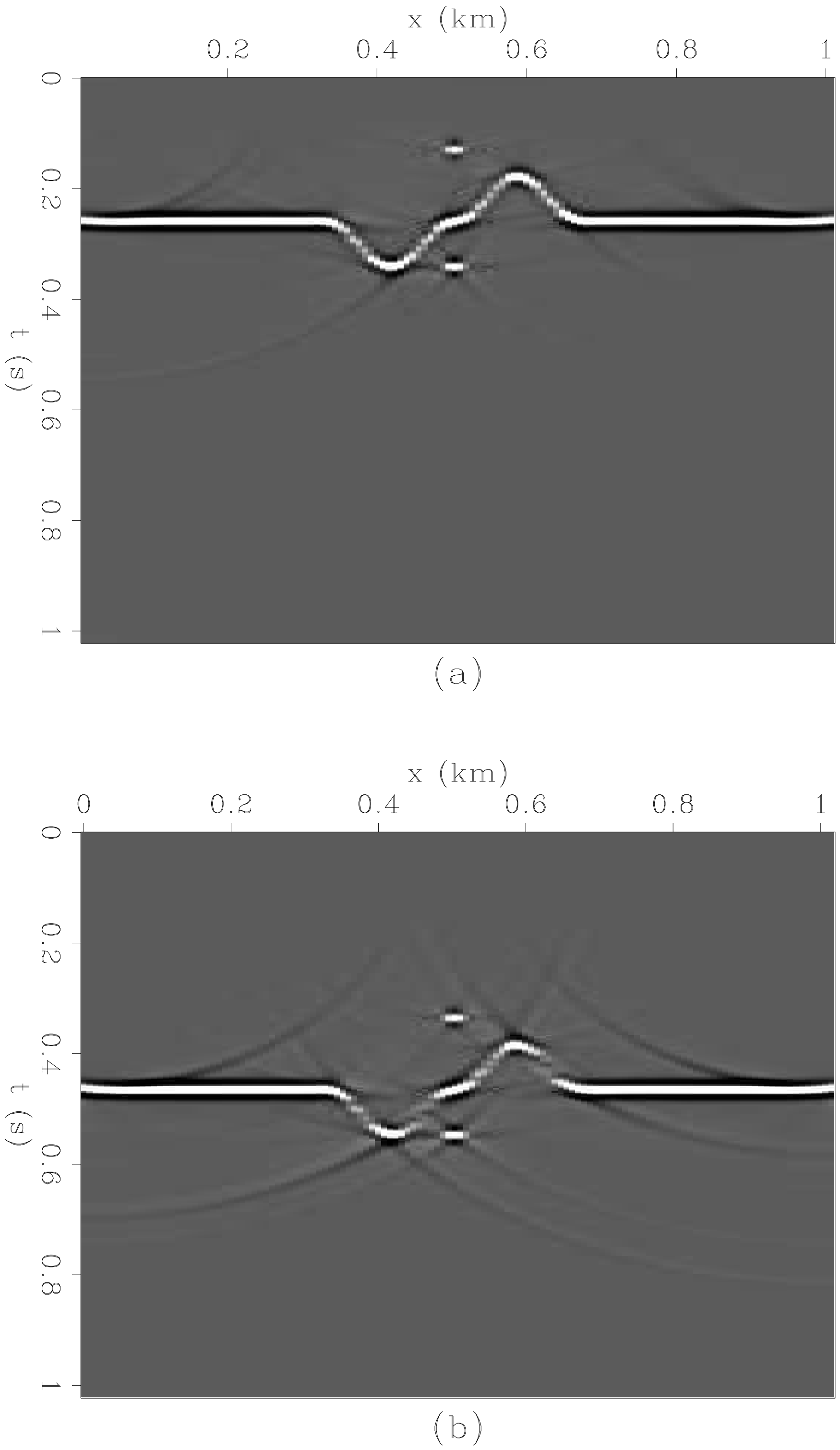

Figure 9: (a) Wave-equation extrapolation downward followed by migration and (b) wave-equation extrapolation upward followed by migration. dimitri4-syndatum [ER]

Pre-Stack Wave-Equation Datuming

When the subsurface velocity structure is unknown upward continuation must be performed pre-stack. Pre-stack datuming is done by extrapolating the shots and the geophones separately using equation (2) (Berryhill, 1984). Once the data have been upward continued to a flat datum, velocity analysis or any other wave based processing algorithm can be applied.

The model used to generate the pre-stack synthetic data is displayed in Figure 10. The subsurface consists of two point diffractors under a topography which is more complicated than for the zero-offset case. The synthetic shot gather is generated using a pre-stack Kirchhoff routine with the shot placed directly above the diffractors at the top of the mountain. The effects of topography are clearly visible as undulations and discontinuities in the nonhyperbolic diffraction curves of Figure 11a.

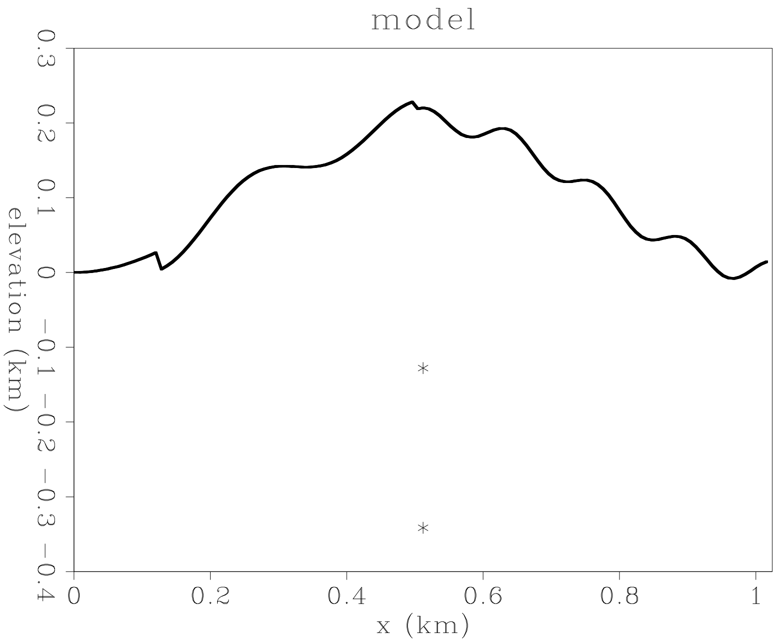

Figure 10: Topography and subsurface structure used to generate the pre-stack synthetic data. dimitri4-shotmodel [ER]

Upward continuing the geophones to a planar datum above the mountain results in hyperbolic trajectories (Figure 11b). The moveout along these curves can now be used to determine the subsurface velocity structure. Some of the sharp features in the topography cause artifacts which are visible as diffractions after the main events. These artifacts would not add constructively in the velocity analysis.

DISCUSSION AND CONCLUSION

In the preceding section I demonstrated that wave-equation extrapolation is superior to static shift when raypaths are not vertical. This conclusion in itself is not new and has been demonstrated by other authors (Wiggins, 1984; Shtivelman and Canning, 1988; Reshef, 1991). None of these authors discuss the determination of the velocity

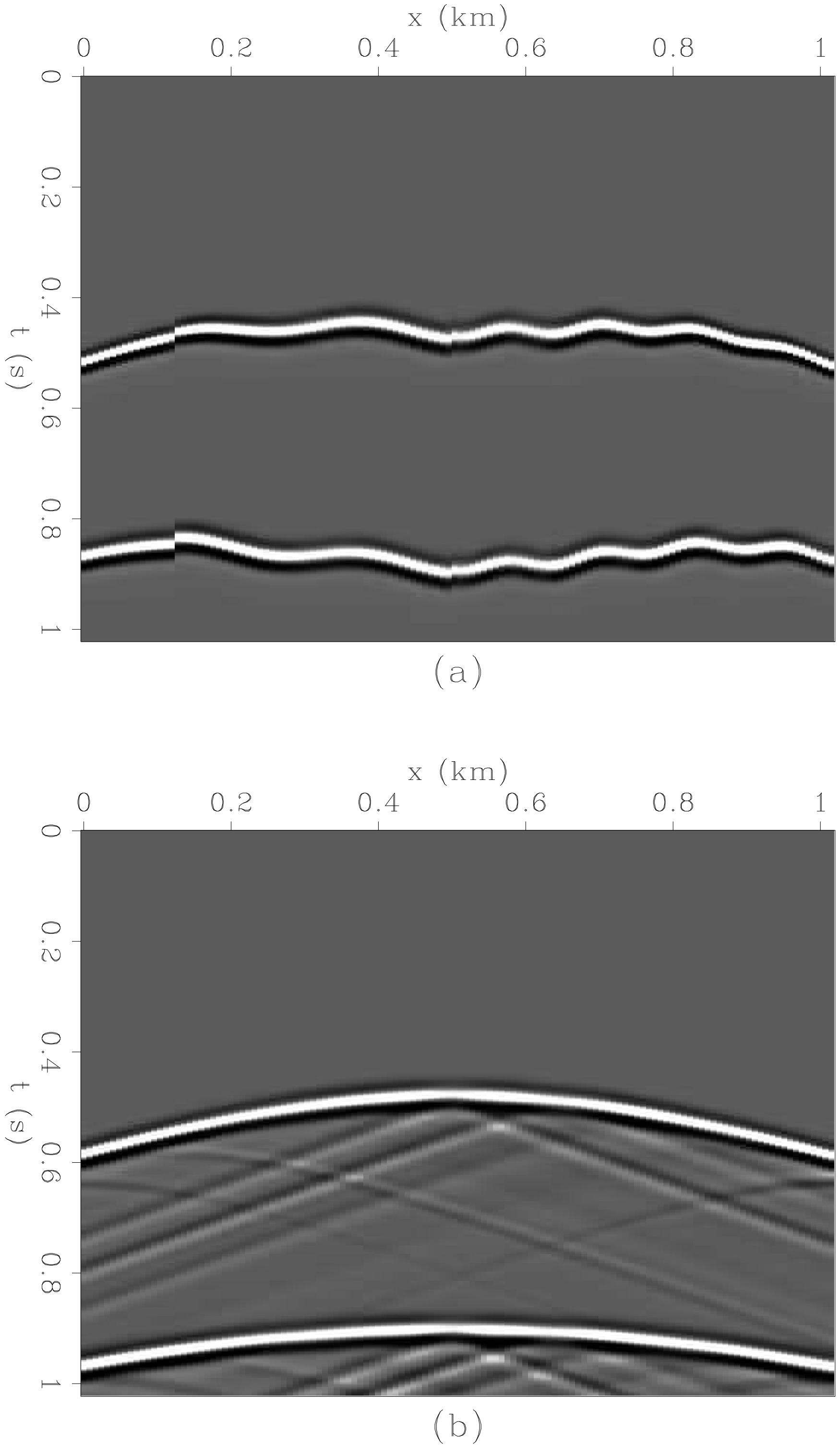

Figure 11: (a) Synthetic shot gather distorted by the irregular surface topography. (b) Continuing the geophones to a level datum above the topography eliminates the distortions and produces hyperbolic moveout trajectories. dimitri4-shotsyn [ER]

to be used in the datuming algorithm at any great length. In regions of large topographic relief the subsurface velocity structure is difficult to determine, therefore it may not always be possible to continue the data to some lower datum directly. I have shown that it is feasible to continue data upwards and perform wave-equation based processing at the new flat datum. Although I show this for time migration, the same logic indicates that velocity analysis, DMO, or pre-stack migration could be applied at the higher datum.

Some resolution of steep dips is lost due to loss of aperture as the wavefield is extrapolated upward. This suggests that it may be adequate to perform the datuming by finite-differencing with the 15° or 45° equations. This may be particularly applicable if it is desired to downward continue the data after the subsurface velocity structure has been determined because the finite-difference formulation allows lateral velocity variation.

Because the Kirchhoff datuming algorithm can be formulated as conjugate pairs for upward and downward continuation, it is possible to formulate re-datuming as a least-squares minimization problem using the conjugate-gradient descent method. This is done by Ji and Claerbout (1992) for a frequency domain datuming scheme using the same concept as Reshef (1991). Popovici (1992) formulates $v(x, z)$ datuming in the frequency domain as upward and downward conjugate pairs which could also be used in a conjugate-gradient scheme. The use of such least-squares datuming may improve the method by eliminating artifacts such as those visible in Figure 11b. Least-squares datuming may also improve results where aperture is limited, particularly in pre-stack datuming.

No matter what the datuming algorithm is based on (Kirchhoff, Fourier, or finite-difference), my proposed application can be outlined in three major steps:

- Extrapolate the data upwards to a flat datum This eliminates the distortions caused by the irregular acquisition topography.
- Perform velocity analysis at the flat datum. This determines the near-surface velocity structure.
- Either perform the processing and imaging at the upper datum or extrapolate downward to some flat datum below the acquisition topography.

The next phase in this investigation is to apply wave-equation datuming to an actual land data set with irregular acquisition topography.

REFERENCES

Berryhill, J. R., 1979, Wave equation datuming: Geophysics, **44**, no. 8, 1329–1344.

Berryhill, J. R., 1984, Wave equation datuming before stack (short note): Geophysics, **49**, no. 11, 2064–2067.

Berryhill, J. A., 1986, Submarine canyons - velocity replacement by wave equation datuming before stack: Geophysics, **51**, no. 8, 1572–1579.

Bevc, D., 1992, Wave-equation extrapolation of land data with irregular acquisition topography: SEP–**73**, 301–304.

Claerbout, J. F., 1992, Anti aliasing: SEP–**73**, 371–390.

Fowler, P., 1988, Seismic velocity estimation using prestack time migration: SEP–**58**.

Ji, J., and Claerbout, J. F., 1992, Phase shift datuming and migration from an irregular surface: SEP–**75**, 157–170.

McMechan, G. A., and Chen, H. W., 1990, Implicit static corrections in prestack migration of common-source data: Geophysics, **55**, no. 6, 757–760.

Popovici, A. M., 1992, Wave-equation datuming in variable velocity media: SEP–**75**, 191–214.

Reshef, M., 1991, Depth migration from irregular surfaces with depth extrapolation methods (short note): Geophysics, **56**, no. 1, 119–122.

Schneider, W. A., 1978, Integral formulation for migration in two-dimensions and three-dimensions: Geophysics, **43**, no. 1, 49–76.

Shtivelman, V., and Canning, A., 1988, Datum correction by wave equation extrapolation: Geophysics, **53**, no. 10, 1311–1322.

Wiggins, J. W., 1984, Kirchhoff integral extrapolation and migration of nonplanar data: Geophysics, **49**, no. 8, 1239–1248.

Yilmaz, O., and Lucas, D., 1986, Prestack layer replacement: Geophysics, **51**, no. 7, 1355–1369.

Zhang, L., and Claerbout, J. F., 1992, Wave-equation resampling of unevenly spaced traces: SEP–**75**, 243–250.

APPENDIX A

In this Appendix I review the derivation of the expression for upward continuation of a scalar wavefield given by Berryhill (1979).

The Kirchhoff integral equation (Schneider, 1978) may be written for an up-going scalar wavefield $U(x, y, z, t)$ as

$$U(x,y,z,t) = \frac{1}{2\pi}\int dA \frac{\cos\theta}{r^2}\left[U(x_0,y_0,z_0,t-\frac{r}{c}) + \frac{r}{c}\frac{\partial}{\partial t}U(x_0,y_0,z_0,t-\frac{r}{c})\right] \quad \text{(A-1)}$$

where the wavefield is known for all points (x_0, y_0, z_0) and for all time on the planar surface A. By performing the two-dimensional integral the wavefield can be expressed at any point above the planar surface.

If the wavefield is only known along a line in the plane and is assumed to be independent of the coordinate perpendicular to this line, the integration can be carried out over the perpendicular coordinate. The geometry of this situation is illustrated in Figure A-A-1 where the wave field is recorded along the x direction and is assumed to be constant in the y direction. Following Berryhill (1979) the integral over dA is performed for an observation point $U(0, z, t)$ directly above the origin of the coordinate axes:

$$U(0,z,t) = \frac{1}{2\pi}\int_{-\infty}^{\infty} dx\; z\int_{-\infty}^{\infty} dy \frac{1}{r^3}\left[U(x,0,t-\frac{r}{c}) + \frac{r}{c}\frac{\partial}{\partial t}U(x,0,t-\frac{r}{c})\right] \tag{A-2}$$

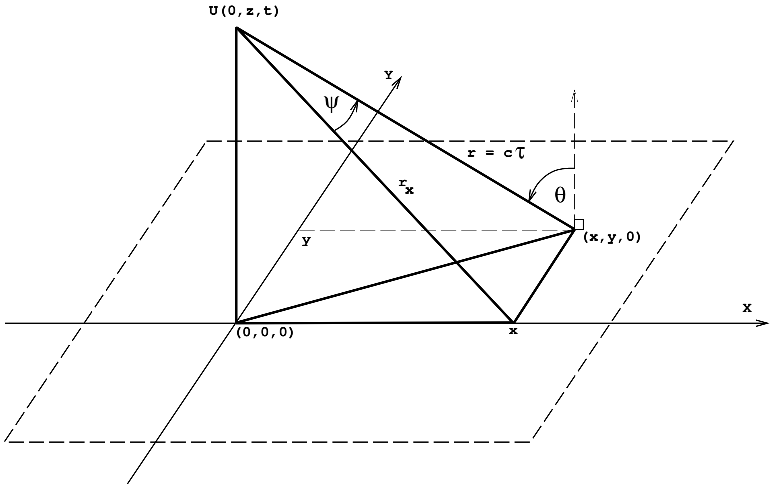

Figure A-1: Geometry for the upward continuation of a wavefield. dimitri4-datumfig1 [NR]

In order to do the integration in the y direction the following substitutions can be made according to Figure A-A-1:

$$\tau = \frac{r}{c} \qquad r_x = \sqrt{x^2+z^2}$$

$$y = \pm\sqrt{c^2\tau^2 - r_x^2} \qquad dy = \pm\frac{c^2\tau d\tau}{\sqrt{c^2\tau^2 - r_x^2}}$$

Thus the integration in y can be expressed as an integration in τ:

$$\int_{-\infty}^{\infty} dy \longrightarrow 2\int_{\frac{r_x}{c}}^{\infty} d\tau = 2\int_{-\infty}^{\infty} H(\tau - \frac{r_x}{c})$$

where H is the Heavyside function. Inserting these substitutions into equation (A-2):

$$\begin{aligned} U(0,z,t) &= \frac{1}{\pi}\int_{-\infty}^{\infty} dx \frac{z}{c}\int_{-\infty}^{\infty} d\tau H(\tau - \frac{r_x}{c})\cdot \\ &\quad \frac{1}{\tau^2}\frac{1}{\sqrt{\tau^2 - \frac{r_x^2}{c^2}}}\left[U(x,0,t-\tau) + \tau\frac{\partial}{\partial t}U(x,0,t-\tau)\right] \end{aligned} \tag{A-3}$$

Equation (A-A-3) is of the form of a convolution in time. For reference I write the general form of the convolution integral as:

$$\int_{-\infty}^{\infty} f(t-\tau)g(\tau)d\tau = f(t) * g(t)$$

where $f(t-\tau)$ corresponds to $U(t-\tau)$. Defining

$$G(\tau) = H(\tau - \frac{r_x}{c}) \left[\frac{1}{\tau^2} \frac{1}{\sqrt{\tau^2 - \frac{r_x^2}{c^2}}} \right]$$

Equation (A-A-3) can now be written as (looking only at the time part):

$$U(0,z,t) \propto \int_{-\infty}^{\infty} d\tau G(\tau) \left[U(x,0,t-\tau) + \tau \frac{\partial}{\partial t} U(x,0,t-\tau) \right]$$

noting that:

$$U(x,0,t) * \left[H(t - \frac{r_x}{c}) \frac{1}{t^2 \sqrt{t^2 - \frac{r_x^2}{c^2}}} \right] = \frac{dU(x,0,t)}{dt} * \left[H(t - \frac{r_x}{c}) \frac{c^2 \sqrt{t^2 - \frac{r_x^2}{c^2}}}{t r_x^2} \right]$$

and

$$\frac{d}{dt} \left[H(t - \frac{r_x}{c}) \frac{c^2 \sqrt{t^2 - \frac{r_x^2}{c^2}}}{t r_x^2} \right] = H(t - \frac{r_x}{c}) \frac{1}{t^2 \sqrt{t^2 - \frac{r_x^2}{c^2}}}$$

Equation (A-A-3) can now be written as:

$$\begin{aligned} U(0,z,t) &= \frac{1}{\pi} \int_{-\infty}^{\infty} dx \frac{z}{c^2} \frac{dU(x,0,t)}{dt} * H(t - \frac{r_x}{c}) \cdot \\ & \left[\frac{c^2 \sqrt{t^2 - \frac{r_x^2}{c^2}}}{t r_x^2} + \frac{1}{t^2 \sqrt{t^2 - \frac{r_x^2}{c^2}}} \right] \end{aligned} \quad \text{(A-4)}$$

summing the terms in brackets and using the definition of the angle ψ from Figure A-A-1 where

$$\tan \psi = \frac{\sqrt{c^2 t^2 - r_x^2}}{r_x} \quad \text{(A-5)}$$

The integrand in equation (A-A-4) can be written as

$$\begin{aligned} Q(t - \frac{r_x}{c}) &= \frac{dU(x,0,t)}{dt} * \left[H(t - \frac{r_x}{c}) \frac{d \tan \psi}{dt} \right] \\ &= U(x,0,t) * \left[H(t - \frac{r_x}{c}) \frac{d^2 \tan \psi}{dt^2} \right] \end{aligned} \quad \text{(A-6)}$$

Finally the expression for the upward continued wavefield is written as

$$U(0,z,t) = \frac{1}{\pi} \int_{-\infty}^{\infty} dx \frac{z}{c} \frac{1}{r_x} Q(t - \frac{r_x}{c}) \quad \text{(A-7)}$$

This is equation (1) of the main text.

For a wavefield transformation from one datum $U(x, z = z_1, t)$ to another $U(x, z = z_2, t)$ the discrete form of equation (A-7) is a summation. Each individual trace $U_j(t)$ comprising $U(x, z = z_2, t)$ is calculated by performing the sum:

$$U_j(t) = \sum_j \triangle x_i \cos\theta_i \frac{t_i}{r_i} Q_i(t - t_i) \tag{A-8}$$

where $Q_i(t-t_i)$ is a filtered input trace recorded at location i and delayed by traveltime t_i. This filtering is performed according to equation (A-A-6). $\triangle x_i$ is the input trace interval, θ_i is the angle between the normal to the surface at $z = z_2$ and the line r_i connecting U_j and U_i. The geometry of the transformation is illustrated in Figure 1 of the main text.

The effect of the filtering operation implied by equation (A-A-6) is to perform a phase-shift of the traces input to the datuming algorithm. This is illustrated in Figure A-2. The input trace is convolved with the second derivative of $\tan\psi$ to produce the output trace which goes into the summation of equation (A-8). The $\tan\psi$ filter is tapered to eliminate undesirable truncation effects.

For downward continuation, the input traces are crosscorrelated with the $\tan\psi$ filter after the summation of equation (A-8) has been performed on the unfiltered traces.

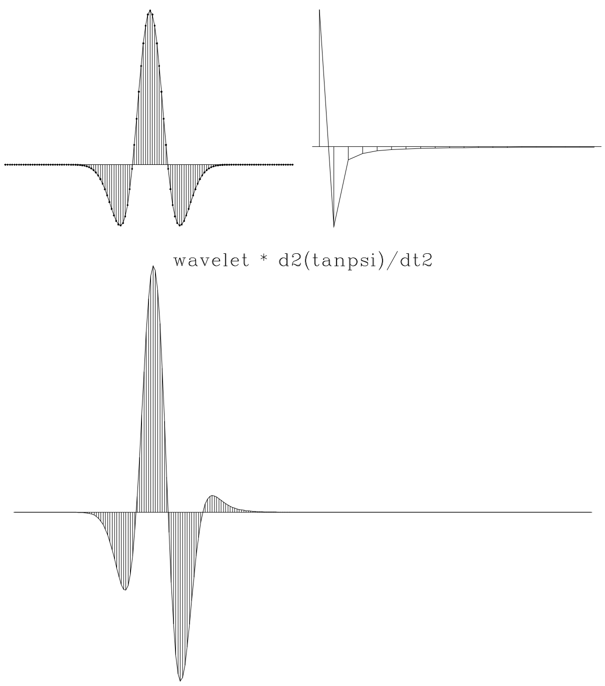

Figure A-2: The wavelet (upper left) is convolved with the second derivative of $\tan\psi$ (upper right) to yield the phase shifted trace (bottom). dimitri4-quedemo [ER]